Electronic structure and magnetic couplings in anatase TiO₂:V codoped with N, F, Cl

Dan Huang[1]**, Yu-Jun Zhao**[2]**, Di-Hu Chen**[1] **and Yuan-Zhi Shao**[1]

[1] School of Physics and Engineering, Sun Yat-sen University, Guangzhou 510275,
People's Republic of China
[2] Department of Physics, South China University of Technology, Guangzhou 510640,
People's Republic of China

E-mail: zhaoyj@scut.edu.cn

Abstract
Using first-principles calculations, we have discussed the stability of the defect charge state and magnetic properties of V_{Ti} defects in anatase TiO₂. While N, F, and Cl are typical nonmetal dopants for photocatalytic activity enhancement of TiO₂, their influence on the magnetism of TiO₂:V is also investigated. We find that V_{Ti}^+ (i.e. V^{5+}) would be favored in the p-type region and V_{Ti}^0 (i.e. V^{4+}) and V_{Ti}^- (i.e. V^{3+}) would be stable in the n-type region. It is demonstrated that while V^{5+} does not carry any local moment, both V^{4+} and V^{3+} defects are preferred to ferromagnetic ordering. Thus, n-type dopants (such as F and Cl) in TiO₂:V samples, which could stabilize V as V^{3+}, are suggested for their many applications requiring combined magnetic and optical functionality, while p-type dopants (such as N) are not suggested.

(Some figures in this article are in colour only in the electronic version)

1. Introduction

Since the discovery of room-temperature ferromagnetism in Co doped anatase TiO₂ [1], numerous experimental investigations [2–7] and theoretical predictions [8–12] have been conducted on the transition metal (such as V, Cr, Mn, Fe, Co etc) doped TiO₂ for a practical diluted magnetic semiconductor (DMS). DMS holds promise for the next revolution of electronic devices with integration of magnetism into traditional semiconductor technology. Meanwhile, TiO₂ is a widely used photocatalytic material due to its unique optical and electronic properties, and low cost [13]. Anatase TiO₂ exhibits a photocatalytic activity only under ultraviolet light illumination as it has a wide band gap of 3.2 eV [14]. In order to enhance its photocatalytic activity under visible light illumination, TiO₂ samples are often doped with nonmetal atoms, such as N [13, 15], F [16, 17], Cl [18], etc, aimed at shifting the optical absorption edge to lower energies. Nb and Ta doped TiO₂ also could be used as a transparent conducting oxide (TCO) [19, 20] or a thermoelectric (TE) material [21]. Titanium dioxide has attracted much attention recently as an emerging multi-functional material.

In particular, vanadium doped TiO₂ has been demonstrated with both room-temperature ferromagnetism [2, 3] and visible light photocatalytic activity [22, 23]. As a promising DMS material, V doped TiO₂ has shown interesting magnetic properties. For instance, Hong *et al* [2] reported experimentally that they obtained single phased anatase TiO₂:V with unexpectedly large magnetic moments of about $4.2\mu_B/V$. Tian *et al* [3] found the ferromagnetism was enhanced after postannealing the samples in argon atmosphere. From the theoretical aspect, He *et al* [8] reported that the total magnetic moments have a giant increase with the formation of an oxygen vacancy. Du *et al* [9] found the ferromagnetism in TiO₂:V originated from a combination of short-range superexchange coupling and long-range bound magnetic polaron percolation. Recently, Osorio-Guillén *et al* [24] explained the ferromagnetism in TiO₂:V and the conductivity in TiO₂:Nb,Ta by a simple picture according to the position of the atomic d-orbital energies of the early transition-metal dopant. Since the highest occupied atomic d-orbital of vanadium is energetically lower than that of titanium, V_{Ti}^0 is expected to have an open-shell d-level electronic configuration and carry local magnetic moments. All of the above theoretical calculations mainly focused on the
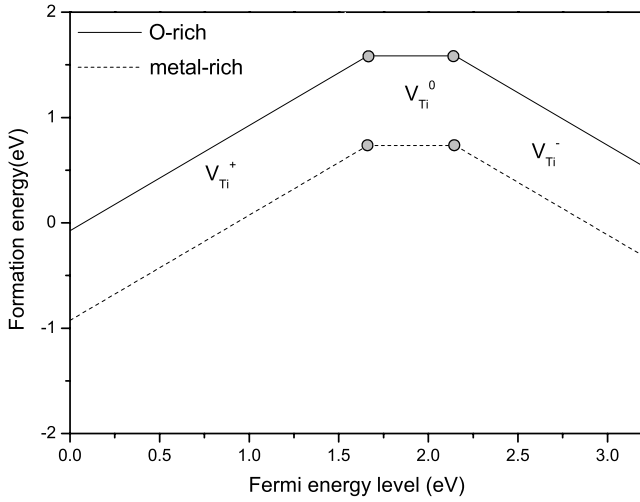
Figure 1. The formation energy of substitutive V defects in TiO$_2$ under metal-rich and O-rich conditions. The defect charge states of the defects are marked accordingly. Here the experimental gap of anatase TiO$_2$, $E_g = 3.2$ eV is adopted.

substitutional vanadium defect with neutral defect charge state, V_{Ti}^0 (i.e. V^{4+}), which is expected to carry only $1\mu_B/V$ spin moment, significantly less than the experimentally observed magnetic moments. According to the experiments, however, there are reports on the mixing of valence states of V^{3+} and V^{4+} [22], or V^{4+} and V^{5+} [23] in the TiO$_2$:V samples observed by x-ray photoelectron spectroscopy (XPS). It is obvious that V_{Ti}^+ (i.e. V^{5+}) does not possess of any d-electrons, thus no local magnetic moment is expected. The magnetic moment and couplings are expected to be remarkably different for vanadium defects with different charge states, which will also be affected by the codoping of nonmetals (N, F, Cl, etc) for improving the photocatalytic activity. Here, we will focus on the possible electronic structure and the magnetic properties of TiO$_2$:V samples *with and without* codoping of N, F, and Cl.

Based on first-principles calculations, we find in this work that V_{Ti}^+ (i.e. V^{5+}), is preferred in a p-type sample, which may

not be possessed of any magnetic property. Both V_{Ti}^0 (i.e. V^{4+}) and V_{Ti}^- (i.e. V^{3+}) stabilized with ferromagnetic (FM) coupling could be preferred in n-type samples. In the F, Cl, or N codoped TiO$_2$:V systems, we find that ferromagnetism is enhanced in TiO$_2$:V by F and Cl (n-type dopants) codoping, but may be depleted by N codoping (p-type dopant). This indicates that n-type dopants (such as F and Cl) are suggested to improve the photocatalytic activity in TiO$_2$:V for its variety of applications requiring combined magnetic and optical functionality.

2. Computational details

Our first-principles calculations have been carried out with the spin polarized density functional theory (DFT) and the PW91 generalized gradient approximation (GGA) formulism [25] for the exchange and correlation functional. A plane-wave basis set and the projector augmented wave potentials [26] are employed as implemented in the Vienna *ab initio* simulation package (VASP) [27, 28]. An energy cutoff of 500 eV is used throughout the calculations. Brillouin zone integrations are performed with the special k-point method over a Gamma centered $4 \times 4 \times 4$ Monkhorst–Pack mesh for a supercell consisting of $2 \times 2 \times 1$ unit cells (48 atoms). The theoretically calculated equilibrium lattice parameters of anatase TiO$_2$, $a = 3.829$ Å, $c = 9.614$ Å are employed, and the internal coordinates are fully relaxed throughout this work.

3. Results and discussion

3.1. Stability of V_{Ti} defect charge states

The formation enthalpies for V substituting Ti at different charge states are calculated with a single V atom in a $2 \times 2 \times 1$ supercell consisting of 48 atoms according to [29]

$$\Delta H_f^{(\alpha,q)} = E(\alpha, q) - E(0) + \sum_\alpha n_a(\Delta\mu_\alpha + \mu_\alpha^{solid})$$
$$+ q(E_{VBM} + E_F), \qquad (1)$$

where $E(\alpha, q)$ and $E(0)$ are the total energy of the supercells with and without defects α. Here $(\Delta\mu_\alpha + \mu_\alpha^{solid})$ is the absolute
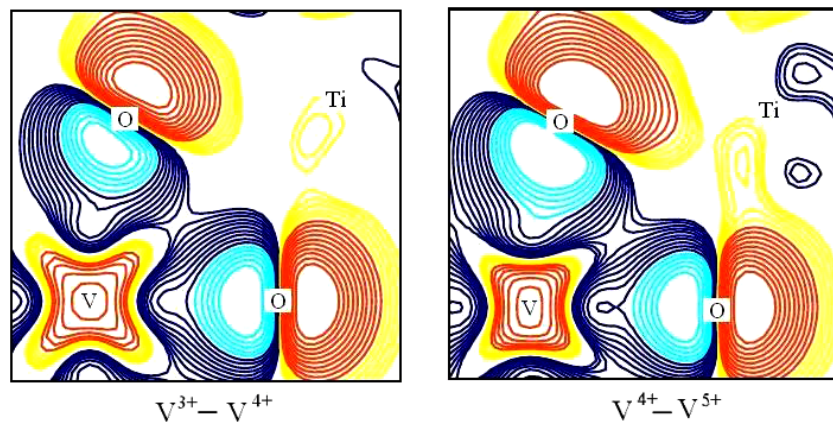

Figure 2. The difference of charge density between V^{3+} and V^{4+}, and V^{4+} and V^{5+} in the (100) plane. The red and yellow lines (loops at the right or up side of the O atoms, as well as around the V atom) stand for charge accumulation, while the blue and cyan lines (loops around the left or down side of the O atoms) stand for charge depletion. The charge density contours start at $0.01e$ Å^{-3} and increase or decrease successively by a factor of $2^{1/3}$.
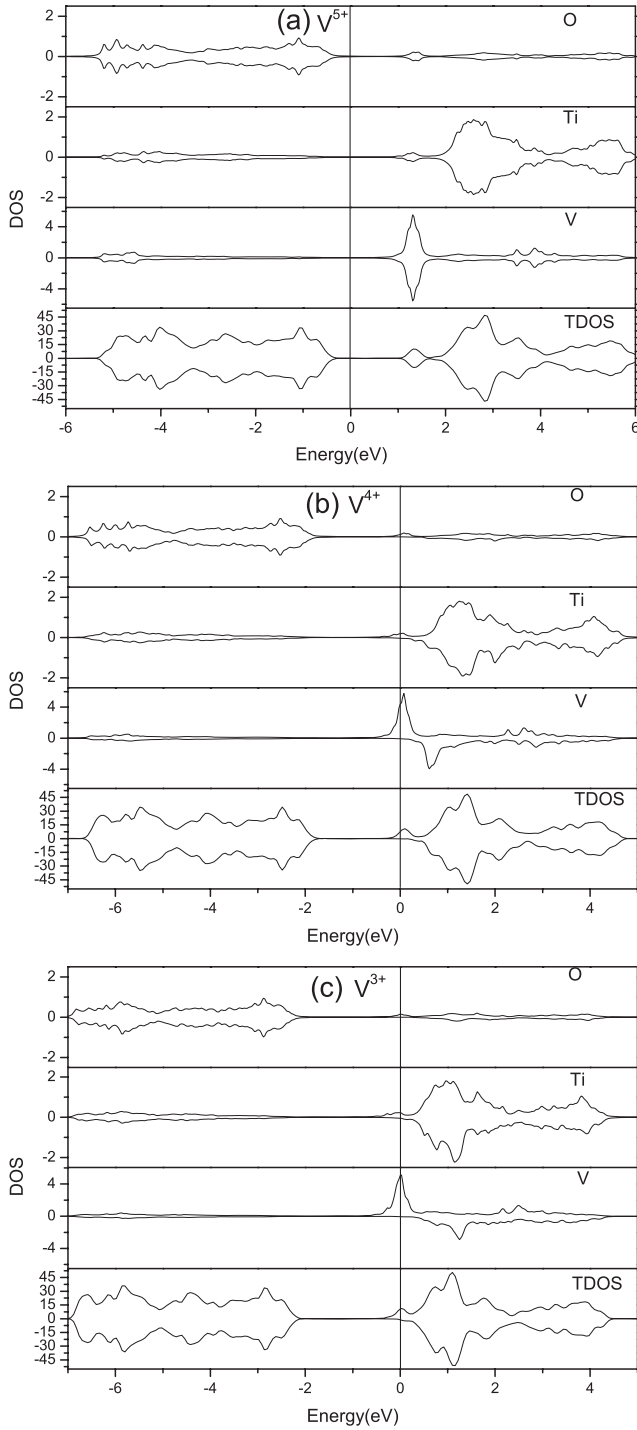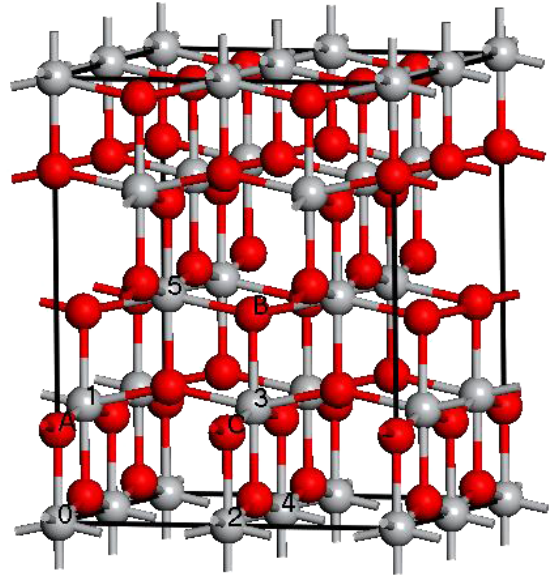
Figure 4. The schematic 48-atom supercell used in the calculations. The gray and red balls (gray and dark balls in the printed edition, respectively) stand for Ti and O atoms, respectively.

Owing to the finite supercell used in our calculation, we have applied the image charge correction to correct the energy of the charged supercell. Recently, Lany and Zunger [30] found that the formation energy of $GaAs:V_{As}^{3+}$ could be well-converged in fairly small supercells such as a 64-atom or even 32-atom supercell, as long as the potential alignment and image charge correction are included. We also consider the potential alignment between the doped systems and the defect-free system by adding ΔV into the $(E_{VBM} + E_F)$ term, where ΔV is the electrostatic alignment between the doped host and the pure host.

In order to preclude the formation of Ti_2O_3 in TiO_2, we set $\Delta\mu_{Ti} + 2\Delta\mu_O = \Delta H_f(TiO_2) = -10.09$ eV and $2\Delta\mu_{Ti} + 3\Delta\mu_O \leqslant \Delta H_f(Ti_2O_3)$ (calculated to be -16.29 eV). Thus, $\Delta\mu_{Ti} = -2.10$ eV (i.e. $\Delta\mu_O = -3.99$ eV) is found to be the upper limit of the chemical potential of titanium during TiO_2 growth. Under the metal-rich condition, we set $\Delta\mu_V = -0.54$ eV to avoid precipitation of V_2O_3 ($\Delta H_f(V_2O_3) = -13.04$ eV). Under the oxygen-rich condition, we set $\Delta\mu_O = 0$, referring to the O chemical potential in molecule O_2 (μ_o). Correspondingly, $\Delta\mu_{Ti} = -10.09$ eV is derived from $\Delta\mu_{Ti} + 2\Delta\mu_O = \Delta H_f(TiO_2)$, and $\Delta\mu_V = -9.37$ eV is the maximum chemical potential of vanadium under the constriction of $2\Delta\mu_V + 5\Delta\mu_o \leqslant \Delta H_f(V_2O_5) = -18.74$ eV.

It is well-known that the band gap is usually underestimated by LDA and GGA due to the delocalization error and static correlation error of commonly used approximations [31]. The calculated GGA band gap is 1.84 eV, which is significantly smaller than the experimental value of 3.2 eV. Without any energy gap correction, our calculated transition energy levels for V^{5+}/V^{4+} and V^{4+}/V^{3+} are 1.67 eV and 2.15 eV, respectively. The calculation of transition levels is involved with the total energies through the formation energy. Typically, the total energy calculations and the charge density are

Figure 3. The total density of state (DOS) of $TiO_2{:}V$ and projected DOS for O, Ti, and V under different defect charge states: (a) V^{5+}, (b) V^{4+}, and (c) V^{3+}.

value of the chemical potential of atom α. μ_α^{solid} is defined as the chemical potential of the elemental solid. Also n_α is the number of atoms for each defect; $n_\alpha = -1$ if an atom is added, while $n_\alpha = 1$ if an atom is removed. E_{VBM} represents the energy of the valence band maximum (VBM) of the defect-free system and E_F is the Fermi energy relative to the E_{VBM}. For charged systems, a compensating homogeneous jellium background charge is assumed to preserve overall neutrality.
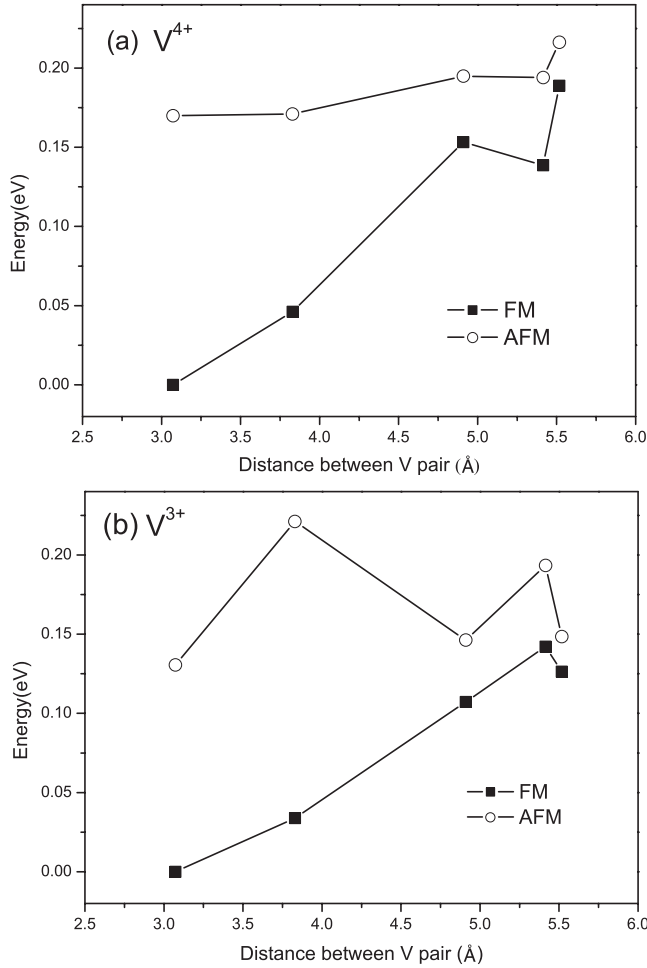
Figure 5. The relative value of E_{fm} and E_{afm} under different charge defect states (a) V^{4+} and (b) V^{3+} with different pair configuration, the minimum is set as zero.

conducted with special k-points or equivalent k-points in the Brillouin zone integration. Therefore, the donor levels, especially those outside the LDA or GGA *k-point weighted* band gap, should be corrected. Here, we assume that the eigenvalues for conduction band states are shifted accordingly as the GGA band gap is corrected to the experimental value. The adopted k-point weighted GGA band gap is 2.25 eV, in good agreement with that obtained in an earlier work by Na-Phattalung *et al* (2.32 eV) [32]. This treatment keeps the transition energy level of V^{4+}/V^{3+} within the band gap, although it is beyond the directly calculated GGA band gap. We notice that the V^{3+} state is observed in the TiO$_2$:V samples experimentally [22]. To confirm the existence of the V^{3+} state, the charge density distributions around the V_{Ti} defect at different charge states are examined. It is found that the electrons around the V atom are remarkably increased as $V^{5+} \rightarrow V^{4+} \rightarrow V^{3+}$ (see in figure 2), indicating that increased numbers of electrons do accumulate around the V_{Ti} defects. This confirms that the vanadium defect could be stable at an oxidation state of +3 in TiO$_2$ and the transition level of V^{4+}/V^{3+} is within the band gap. Therefore, the stable oxidation states of V atoms could be V^{5+}, V^{4+}, and V^{3+} in TiO$_2$:V, which is consistent with the x-ray photoelectron
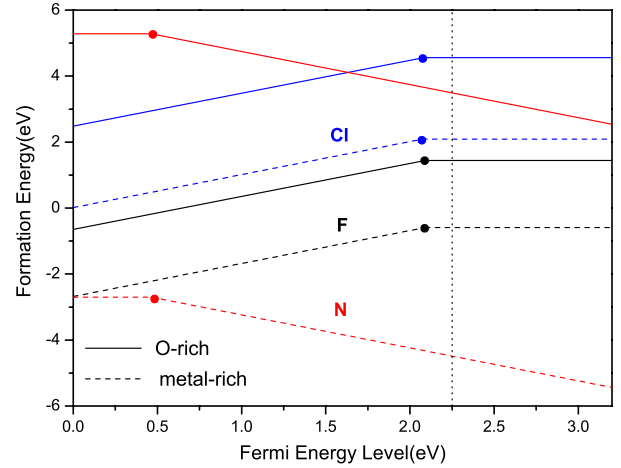

Figure 6. The formation energies of substitutive N (red line), F (black line), and Cl (blue line) defects at O sites in TiO$_2$ under metal-rich and O-rich conditions. Here Cl$_2$ and F$_2$ are adopted as the source for Cl and F doping respectively, while NO is employed for the N doping source. The dotted line indicates the position of the adopted k-point weighted GGA band gap. Here we assume that the eigenvalues for conduction band states, and thus the donor transition levels of F and Cl, are shifted accordingly as the LDA band gap is corrected to the experimental value [35].

spectroscopy results in earlier experiments [22, 23]. and our calculated charge density difference plot in figure 2.

3.2. Magnetic properties of V_{Ti} at various charge states

Our results show that V^{5+} does not possess any local magnetic moment due to the lack of any localized d-electrons. The supercells containing V^{4+} and V^{3+} have $0.938\mu_B$ and $1.644\mu_B$ per vanadium. Since V^{5+} is favored in the p-type region and V^{4+} and V^{3+} are favored in n-type region (figure 1), it is concluded that the n-type TiO$_2$:V is an FM semiconductor while there is no ferromagnetism in p-type samples. Furthermore, the local magnetic moment is expected to increase with the Fermi level moving up to the conduction band minimum.

The densities of states of TiO$_2$:V with different vanadium oxidation states are shown in figure 3. It indicates that the valence band is mainly contributed by O atoms, while the conduction band is mainly contributed by Ti atoms. Clearly, V^{5+} introduces defect states below the conduction band (figure 3(a)). This is consistent with the fact that the vanadium d-orbital energy of the highest occupied atomic d-orbital is lower than that of titanium [24]. When the defect states of the V atom are ionized, there is an exchange splitting in the V d-orbital. Both the majority spin states of V^{4+} and V^{3+} d levels are filled by electrons, and the d-orbital of V maintains the open-shell configuration.

In order to get a clear picture of the magnetic mechanism, we have studied the FM and antiferromagnetic (AFM) coupling for two V_{Ti} defects in various configurations in a $2 \times 2 \times 1$ supercell (figure 4). One V is put at a Ti lattice site (marked 0 in figure 4), and the other V atom is put at positions 1–5 of the Ti lattice sites according to the order of V–V distances. In each case, the energy difference between
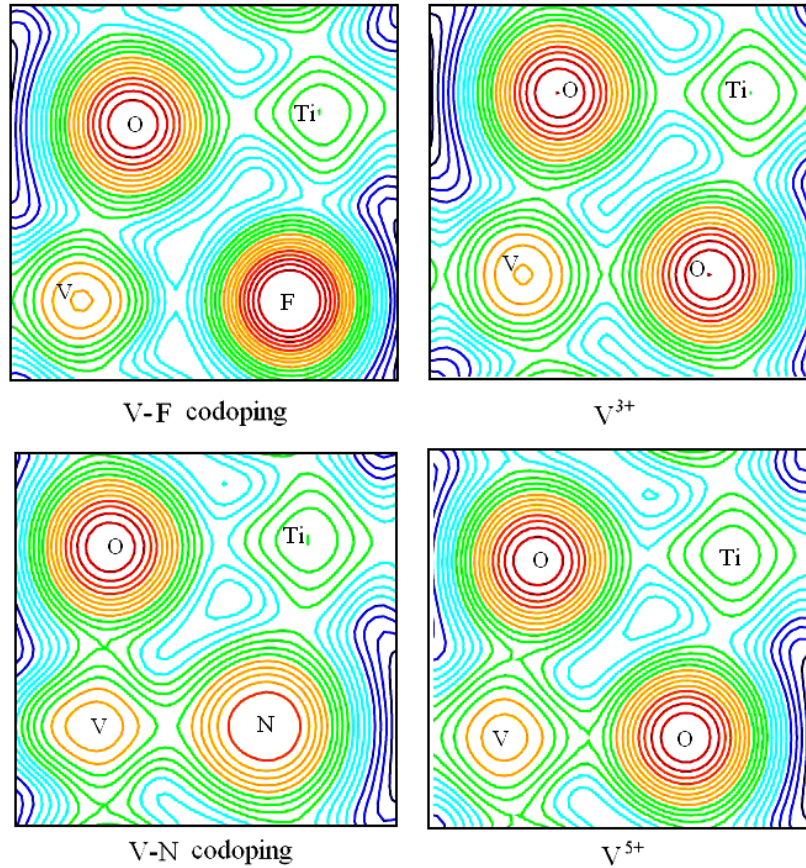
Figure 7. The (100) plane charge density distributions of the codoping supercells. The charge density distributions of V^{3+} and V^{5+} are also shown in order to compare them with the codoped systems. The atom positions are labeled in the plots. The charge density contours start at $0.01e$ Å^{-3} and increase successively by a factor of $2^{1/3}$.

FM and AFM orderings, $\Delta E_{ex} = E_{afm} - E_{fm}$, is calculated for their magnetic coupling preference. Figure 5 shows the relative value of E_{afm} and E_{fm} for the V^{4+} pair and the V^{3+} pair. The favored magnetic coupling is found to be FM for both V^{4+} and V^{3+} pairs in TiO$_2$. The nearest configuration with a FM state has the lowest energy. It indicates that there is a clustering tendency for a V–O–V cluster. This is different from the situation of TiO$_2$:Cr [10], where Cr^{3+} tends to distribute uniformly and leads to paramagnetism, although Cr^{4+} tends to form a Cr–O–Cr cluster with strong ferromagnetism. According to whether the d-orbital near the Fermi energy level is open or closed, the magnetic coupling could be favored for FM or AFM through the hopping interaction [33, 34]. Both of the DOSs of V^{4+} and V^{3+} show the open-shell configuration for the corresponding V_{Ti} defects, which maintains their stable FM coupling.

3.3. TiO$_2$:V codoped with N, F, and Cl

Our results show that the magnetism is favorable in n-type but unfavorable in p-type samples of TiO$_2$:V. The p-type and n-type nonmetal dopants like N, F, Cl are usually used for the enhancement of its photocatalytic activity in TiO$_2$. Figure 6 shows the formation energies of N, F, and Cl substituting at O sites in TiO$_2$ under metal-rich and O-rich conditions. Under metal-rich conditions, the substituting formation energies have

relative low values. V_{Ti} also has a low formation energy under metal-rich conditions (cf figure 1). This indicates that V_{Ti} and N$_O$ (F$_O$, Cl$_O$) could be codoped under metal-rich conditions. In fact, there are experimental reports on transition metal and anion ions in TiO$_2$ [22, 36]. For the potential applications requiring combined magnetic and optical functionality, it is interested to investigate the effect of N, F, or Cl codoping on the magnetic properties of TiO$_2$:V.

To find the configuration of vanadium with the codoping atoms, we put V at position 0 of the Ti lattice site and put the codoped atom at position A (near configuration) or position B (far configuration) of the O lattice site as shown in figure 4. Table 1 lists the relative energies E and the magnetic moments of the codoped configurations. It is shown that the TiO$_2$:V system codoped with p-type dopant N does not carry any local magnetic moment. The TiO$_2$:V system codoped with n-type dopants F and Cl possesses a magnetic moment approximating that of V^{3+}. By comparing the electron density distribution of V defects in the codoped systems with those of V^{5+} and V^{3+} (figure 7), we find that the electron density distribution of V in the F codoped system is very close to that of the V^{3+} defect, while V in the N codoped system is very close to that of the V^{5+} defect. It is clear that the n-type dopants, such as F and Cl, could stabilize V to V^{3+} of the V_{Ti} defects, and a p-type dopant such as N could stabilize V to V^{5+} of no local magnetic moment.

Table 1. The relative energies E and magnetic moments of the N, F, Cl codoped TiO$_2$:V systems. The energies of the near configurations are set to zero.

	N		F		Cl	
	Near	Far	Near	Far	Near	Far
E (eV)	0	0.537	0	0.049	0	0.071
Mag. moment (μ_B/V)	0	0	1.627	1.623	1.472	1.578

Furthermore, we put two codoped nonmetal (F or Cl) atoms in a supercell containing a pair of V ions. The V ions are put at positions 0 and 2 of the Ti lattice sites, while F or Cl atoms are put at positions A and C of the O lattice sites in figure 4, respectively. Our results show that the V pair is stable at the FM state with ΔE_{ex} of 203 meV for F codoping and 96 meV for Cl codoping. Thus, n-type dopants, such as F and Cl, are suggested when TiO$_2$:V samples are prepared for applications requiring combined magnetic and optical functionality. It is clear that the p-type dopants, such as N, will deplete magnetism in the TiO$_2$:V system.

4. Conclusion

In summary, we have theoretically investigated the stability of the defect charge state and magnetic properties of substitutional vanadium in anatase TiO$_2$, as well as the codoping effect with N, F, and Cl for a variety of applications requiring combined magnetic and optical functionality. It is demonstrated that V^{5+} is preferred in p-type samples and V^{4+} and V^{3+} could be stable in n-type samples. V^{5+} may not be possessed of any magnetic property, while both V^{4+} and V^{3+} prefer FM coupling. Thus, the n-type characteristic is favored for anatase TiO$_2$:V when it is designed for multi-functionality applications requiring both its magnetic and optical properties. It is confirmed that n-type dopants, such as F and Cl, are expected to enhance the magnetism and p-type dopants, such as N, will deplete the magnetism in the TiO$_2$:V system.

Acknowledgments

References

[1] Matsumoto Y, Murakami M, Shono T, Hasegawa T, Fukumura T, Kawasaki M, Ahmet P, Chikyow T, Koshihara S and Koinuma H 2001 *Science* **291** 854

[2] Hong N H, Sakai J and Hassini A 2004 *Appl. Phys. Lett.* **84** 2602

[3] Tian Z M, Yuan S L, Yuan S J, Xie H Y, He J H, Wang Y Q, Liu K L and Yin S Y 2008 *Solid State Commun.* **146** 522

[4] Zhang X, Wang W H, Li L Y, Cheng Y H, Luo X G and Liu H 2008 *J. Phys. D: Appl. Phys.* **41** 015005

[5] Mi W B, Jiang E Y and Bai H L 2008 *Acta Mater.* **14** 3511

[6] Meng H J, Hou D L, Jia L Y, Ye X J, Zhou H J and Li X L 2007 *J. Appl. Phys.* **102** 073905

[7] Hu E, von Molnár S, Stampe P A, Kennedy R J and Xin Y 2008 *Appl. Phys. Lett.* **92** 012114

[8] He K H, Zheng G, Chen G, Lü T, Wan M and Ji G F 2007 *Solid State Commun.* **144** 54

[9] Du X S, Li Q X, Su H B and Yang J L 2006 *Phys. Rev. B* **74** 233201

[10] Ye L H and Freeman A J 2006 *Phys. Rev. B* **73** 081304(R)

[11] Chen J, Rulis P, Ouyang L Z, Satpathy S and Ching W Y 2006 *Phys. Rev. B* **74** 235207

[12] Janisch R and Spaldin N A 2006 *Phys. Rev. B* **73** 035201

[13] Asahi R, Morikawa T, Ohwaki T, Aoki K and Taga Y 2001 *Science* **293** 269

[14] Kavan L, Grätzel M, Gilbert S E, Klemenz C and Scheel H J 1996 *J. Am. Chem. Soc.* **118** 6716

[15] Okato T, Sakano T and Obara M 2005 *Phys. Rev. B* **72** 115124

[16] Li D, Haneda H, Labhsetwar N K, Hishita S and Ohashi N 2005 *Chem. Phys. Lett.* **401** 579

[17] Yu J C, Yu J G, Ho W K, Jiang Z T and Zhang L Z 2002 *Chem. Mater.* **14** 3808

[18] Luo H M, Takata T, Lee Y, Zhao J F, Domen K and Yan Y S 2004 *Chem. Mater.* **16** 846

[19] Zhang S X, Dhar S, Yu W, Xu H, Ogale S B and Venkatesan T 2007 *Appl. Phys. Lett.* **91** 112113

[20] Hitosugi T, Furubayashi Y, Ueda A, Itabashi K, Inaba K, Hirose Y, Kinoda G, Yamamoto Y, Shimada T and Hasegawa T 2005 *Japan. J. Appl. Phys.* **44** L1063

[21] Kurita D, Ohta S, Sugiura K, Ohta H and Koumoto K 2006 *J. Appl. Phys.* **100** 096105

[22] Gu D E, Yang B C and Hu Y D 2008 *Catal. Commun.* **9** 1472

[23] Iketani K, Sun R D, Toki M, Hirota K and Yamaguchi O 2004 *Mater. Sci. Eng. B* **108** 187

[24] Osorio-Guillén J, Lany S and Zunger A 2008 *Phys. Rev. Lett.* **100** 036601

[25] Perdew J P and Wang Y 1992 *Phys. Rev. B* **45** 13244

[26] Kresse G and Joubert J 1999 *Phys. Rev. B* **59** 1758

[27] Kresse G and Hafner J 1993 *Phys. Rev. B* **47** 558

[28] Kresse G and Furthmüller J 1996 *Phys. Rev. B* **54** 11169

[29] Persson C, Zhao Y J, Lany S and Zunger A 2005 *Phys. Rev. B* **72** 035211

[30] Lany S and Zunger A 2008 *Phys. Rev. B* **78** 235104

[31] Cohen A J, Mori-Sánchez P and Yang W T 2008 *Science* **321** 792

[32] Na-Phattalung S, Smith M F, Kim K, Du M H, Wei S H, Zhang S B and Limpijumnong S 2006 *Phys. Rev. B* **73** 125205

[33] Mahadevan P, Zunger A and Sarma D D 2004 *Phys. Rev. Lett.* **93** 177201

[34] Zhao Y J, Mahadevan P and Zunger A 2005 *J. Appl. Phys.* **98** 113901

[35] Duan X Y, Zhao Y J and Yao R H 2008 *Solid State Commun.* **147** 194

[36] Li X Y, Wu S X, Xu L M, Liu Y J, Xing X J and Li S W 2008 *J. Appl. Phys.* **104** 093914